GFZ
Helmholtz-Zentrum
POTSDAM

Originally published as:

Dai, C., Guo, J., Shang, K., Shum, C. K., Wang, R. (2018): The effect of Earth's oblateness on the seismic moment estimation from satellite gravimetry. - *Geophysical Journal International*, *213*, 2, pp. 1297—1304.

DOI: http://doi.org/10.1093/gji/ggy056

Geophysical Journal International

Geophys. J. Int. (2018) **213,** 1297–1304
Advance Access publication 2018 February 9
GJI Seismology

doi: 10.1093/gji/ggy056

The effect of Earth's oblateness on the seismic moment estimation from satellite gravimetry

Chunli Dai,[1] Junyi Guo,[1] Kun Shang,[1] C.K. Shum[1,2] and Rongjiang Wang[3]

[1] *Division of Geodetic Science, School of Earth Sciences, The Ohio State University, Columbus, OH* 43210*, USA. E-mail: dai.56@osu.edu*
[2] *Institute of Geodesy and Geophysics, Chinese Academy of Sciences, Wuhan* 430077*, China*
[3] *Physics of Earthquakes and Volcanoes, GFZ German Research Centre for Geosciences, D-*14467 *Potsdam, Germany*

Accepted 2018 February 7. Received 2018 February 6; in original form 2017 November 14

SUMMARY

Over the last decade, satellite gravimetry, as a new class of geodetic sensors, has been increasingly studied for its use in improving source model inversion for large undersea earthquakes. When these satellite-observed gravity change data are used to estimate source parameters such as seismic moment, the forward modelling of earthquake seismic deformation is crucial because imperfect modelling could lead to errors in the resolved source parameters. Here, we discuss several modelling issues and focus on one modelling deficiency resulting from the upward continuation of gravity change considering the Earth's oblateness, which is ignored in contemporary studies. For the low degree (degree 60) time-variable gravity solutions from Gravity Recovery and Climate Experiment mission data, the model-predicted gravity change would be overestimated by 9 per cent for the 2011 Tohoku earthquake, and about 6 per cent for the 2010 Maule earthquake. For high degree gravity solutions, the model-predicted gravity change at degree 240 would be overestimated by 30 per cent for the 2011 Tohoku earthquake, resulting in the seismic moment to be systematically underestimated by 30 per cent.

Key words: Satellite gravity; Time variable gravity; Numerical modelling; Computational seismology; Earthquake source observations.

1 INTRODUCTION

Earthquakes can cause crustal/mantle dilation or compression and solid Earth surface uplift or subsidence, resulting in permanent change in Earth's gravity field. The gravity change caused by earthquakes have been shown to be measurable by the Gravity Recovery and Climate Experiment (GRACE) twin-satellite mission (Tapley *et al.* 2004), which has been producing time-variable global gravity field up to spherical harmonic degree around 60 with monthly sampling rate. The GRACE mission has revolutionized our understanding of Earth's mass redistribution, including the terrestrial hydrologic water circulation, ice-sheet and glacier ablation, oceanography and seismology. By surveying right above the rupture region, although with a coarse spatial and temporal resolution, GRACE data have been more commonly used in contemporary studies to detect coseismic signals for several undersea earthquakes, including the 2004 Sumatra–Andaman earthquake (e.g. Han *et al.* 2006; Wang *et al.* 2012c), the 2010 Maule earthquake (e.g. Han *et al.* 2010, Heki & Matsuto 2010, Wang *et al.* 2012a), and the 2011 Tohoku earthquake (e.g. Han *et al.* 2011, 2013; Matsuo & Heki 2011; Cambiotti & Sabadini 2012; Zhou *et al.* 2012; Wang *et al.* 2012b; Dai *et al.* 2014, 2016; Li & Shen 2015). Moreover, GRACE has also shown its unique contribution to the detection of post-seismic gravity signals (Ogawa & Heki 2007; Han *et al.* 2008, 2014; Panet *et al.* 2010; Tanaka & Heki 2014), since GRACE data can compensate for the shortcoming of seismic data on the detection of aseismic slip and post-seismic slip (Chlieh *et al.* 2007; Han *et al.* 2013).

The gravity gradiometry measurements from Gravity field and steady-state Ocean Circulation Explorer (GOCE; Rummel *et al.* 2004) have also been used for the detection of coseismic signals from the large undersea earthquakes. Fuchs *et al.* (2013) found the coseismic signal of the 2011 Tohoku earthquake using the GOCE-measured vertical gravity gradients at the satellite orbit height. Álvarez *et al.* (2014) demonstrated the correlation between the vertical gravity gradient calculated from the GOCE gravity model with the coseismic slip distribution for the 2010 Maule earthquake.

Furthermore, GRACE data have been used to solve for seismic source parameters, such as seismic moment, fault size, fault location and orientation (dip, rake and strike angles). For example, Han *et al.* (2011) solved for the seismic moment, dip and rake angle of the point source for the 2011 Tohoku earthquake. Wang *et al.* (2012a,b) inverted the GRACE data for the fault length, width and uniform slip of the 2010 Maule and the 2011 Tohoku earthquakes. Cambiotti & Sabadini (2013) estimated all parameters (centroid location and moment tensor) of a point source for the 2011 Tohoku earthquake. Enhancing the spatial resolution by using north component of gravity change (and gravity gradient change) from GRACE, Dai *et al.* (2014) solved for the centroid location, seismic moment, fault width and slip rake angle for the 2011 Tohoku earthquake. For five undersea earthquakes over the last decade, Han *et al.* (2013)

© The Author(s) 2018. Published by Oxford University Press on behalf of The Royal Astronomical Society.

Downloaded from https://academic.oup.com/gji/article-abstract/213/2/1297/4847898 by Bibliothek des Wissenschaftsparks Albert Einstein user on 08 January 2019

solved for the seismic moment tensors of multiple centroids but with the location fixed, and Dai *et al.* (2016) solved for both the location and moment tensor parameters.

For the inversion of source parameters such as seismic moment from GRACE, the accurate modelling of the slip-predicted gravity change is important and incorrect modelling may lead to biases. In this paper, we focus on one modelling deficiency in the forward modelling procedure, that is, the effect of the upward continuation of gravity change from the solid Earth's surface to the Earth's mean equatorial radius accounting for the Earth's oblateness, which has not yet been addressed previously for coseismic studies (e.g. Han *et al.* 2011, 2013; Matsuo & Heki 2011; Cambiotti & Sabadini 2012, 2013; Wang *et al.* 2012b). Swenson &Wahr (2002) examined the effects of including the aspherical component of the Earth's shape when modelling the atmospheric effect on the Earth's temporal gravity field. Li *et al.* (2017) conducted an analysis on the non-negligible Earth's aspherical effect (up to 8 per cent) in GRACE surface mass change estimation. It is also mentioned that recent GRACE mascon solutions had taken account of the aspherical effect, for example, the mascon products from Jet Propulsion Laboratory/Cal. Tech. (Watkins *et al.* 2015), NASA Goddard Space Flight Center (Luthcke *et al.* 2013), which used a proper position of the mass element on the ellipsoidal Earth's surface in calculating the gravitational potential.

In this study, we show that this effect to earthquakes source model inversion is non-negligible, and if ignored, may induce systematic error for the modelled gravity change, and consequently the underestimation for the inverted seismic moment parameter from GRACE. In Section 2, we discuss several modelling issues and elaborate the proper way to mitigate the effect from Earth's oblateness. In Section 3, we numerically evaluate the effect of considering Earth's oblateness for modelling the gravity change of five undersea earthquakes, especially the 2011 Tohoku earthquake, and the 2010 Maule earthquake. Finally, Section 4 concludes the findings.

2 ISSUES IN THE FORWARD MODELLING OF GRAVITY CHANGE

The accurate modelling of the GRACE-commensurable gravity change corresponding to an earthquake source model is a crucial prerequisite for inverting for earthquake source parameters. To introduce and illustrate several modelling problems, we first briefly introduce our forward modelling approach as in (Dai *et al.* 2014) for the slip-predicted gravity change, which is based on dislocation theory in a layered half-space (Wang *et al.* 2006). First, the gravity change and surface displacement at full spatial resolution responding to the solid Earth deformation caused by a rupture, can be evaluated at solid Earth's surface, for example, the ocean floor for undersea earthquakes; Second, the gravity change associated with the passive ocean response (de Linage *et al.* 2009; Cambiotti *et al.* 2011) and the topography effect (Li & Chen 2013) can be estimated; Third, the model-predicted gravity change at the ocean floor is expanded to geopotential spherical harmonic coefficients up to degree 900. Finally, each component of gravity and gravity gradient change is computed on Earth's mean equatorial radius (6378.1363 km) from the geopotential coefficients up to the maximum degree (e.g. degree 60) commensurable with the respective GRACE data products.

During the above modelling procedures, several essential modelling issues have been widely discussed in previous studies:

First is the effect of ocean's response to the seafloor deformation on the gravity change. The passive response of ocean water corresponding to the crustal deformation has been extensively investigated and shown significant influence on the gravity change from the satellite gravimetry (de Linage *et al.* 2009; Heki & Matsuo 2010; Broerse *et al.* 2011; Cambiotti *et al.* 2011; Matsuo & Heki 2011). Broerse *et al.* (2014) revisited the calculation of the ocean response effect, and quantitatively demonstrated the significance of assuming a realistic continents-divided ocean (Dai *et al.* 2014) instead of a globally uniform ocean, showing that the uniform ocean assumption can cause errors in gravity up to 40 per cent for the 2010 Maule earthquake.

The second is the effect of topography/bathymetry variation. The gravity change caused by the horizontal displacement over a sloped topography, referred to as topography effect, has been considered by several researchers (Li & Chen 2013; Broerse *et al.* 2014; Dai *et al.* 2014; Dai 2015; Li *et al.* 2016). Li *et al.* (2016) conduct a comprehensive analysis of the topography effect for the 2011 Tohoku earthquake by estimating the 'equivalent' ocean floor uplift due to the southeast horizontal displacement over the sloped Japan Trench, the sea water compensation effect, the crustal density changes from dilation and compression over an inclined topography, and the effects of horizontal motion at the inclined Moho, and they conclude that the total effect is about 7 per cent of the gravity change by the solid Earth deformation (expressed at a spherical harmonic truncation degree of 60).

The third is the effect of Earth's curvature. Dislocation theory in a half-space Earth model is often used in computing coseismic deformation. The effect of Earth's curvature has been widely studied (e.g. Sun & Okubo 1993; Pollitz 1996; Wang *et al.* 2006) by estimating the differences between flat and spherical Earth models, and claimed as negligible for the near field. Dong *et al.* (2016) revisit the curvature effect using a new approach, which approximates the flat-Earth model by a spherical Earth model with large radius, and they conclude that for shallow earthquakes (depth < 30 km), the effect of the Earth's curvature is generally less than 2 per cent; whereas the curvature effect can be up to 30 per cent when source depth is 600 km, for example, for the 2013 Okhotsk deep-focus earthquake (Tanaka *et al.* 2015).

Before discussing the effect of the Earth's oblateness, we elaborate a little bit on the effect of spherical harmonic truncation. Since GRACE provides gravity data up to a limited spherical harmonic degree, same procedure needs to be carried out for the modelling of gravity change by fault rupture. Broerse *et al.* (2014) conclude that it is important to carry out the spherical harmonic expansion at a high degree even when the application requires a lower one. For the 2011 Tohoku earthquake, Fig. 1(c) shows the gravity change truncated at degree 40, after the spherical harmonic expansion of the modelled gravity change (Fig. 1a) to degree 900. The degree of truncation is selected as 40 based on the localized spectral analysis (Dai *et al.* 2016). The degree variance (Fig. 1b), which is the sum of squares of all coefficients for a given degree, shows that the gravity signal caused by an earthquake has high power at higher degree (e.g. peak value at degree 118). This characteristic explains why the truncated gravity change (up to 18.8 μGal, Fig. 1c) only preserves a small portion (2 per cent) of the modelled gravity change with full resolution, which is as large as 1075 μGal (Fig. 1a).

The spherical harmonic truncation in the modelled gravity is non-negligible even when the Gaussian filter is applied. In order to reduce north-south stripes in GRACE Level 2 products, Gaussian filter (e.g. Jekeli 1981; Wahr *et al.* 1998; Swenson & Wahr 2002; Guo *et al.* 2010) is a widely used technique to smooth the gravity

Downloaded from https://academic.oup.com/gji/article-abstract/213/2/1297/4847898 by Bibliothek des Wissenschaftsparks Albert Einstein user on 08 January 2019

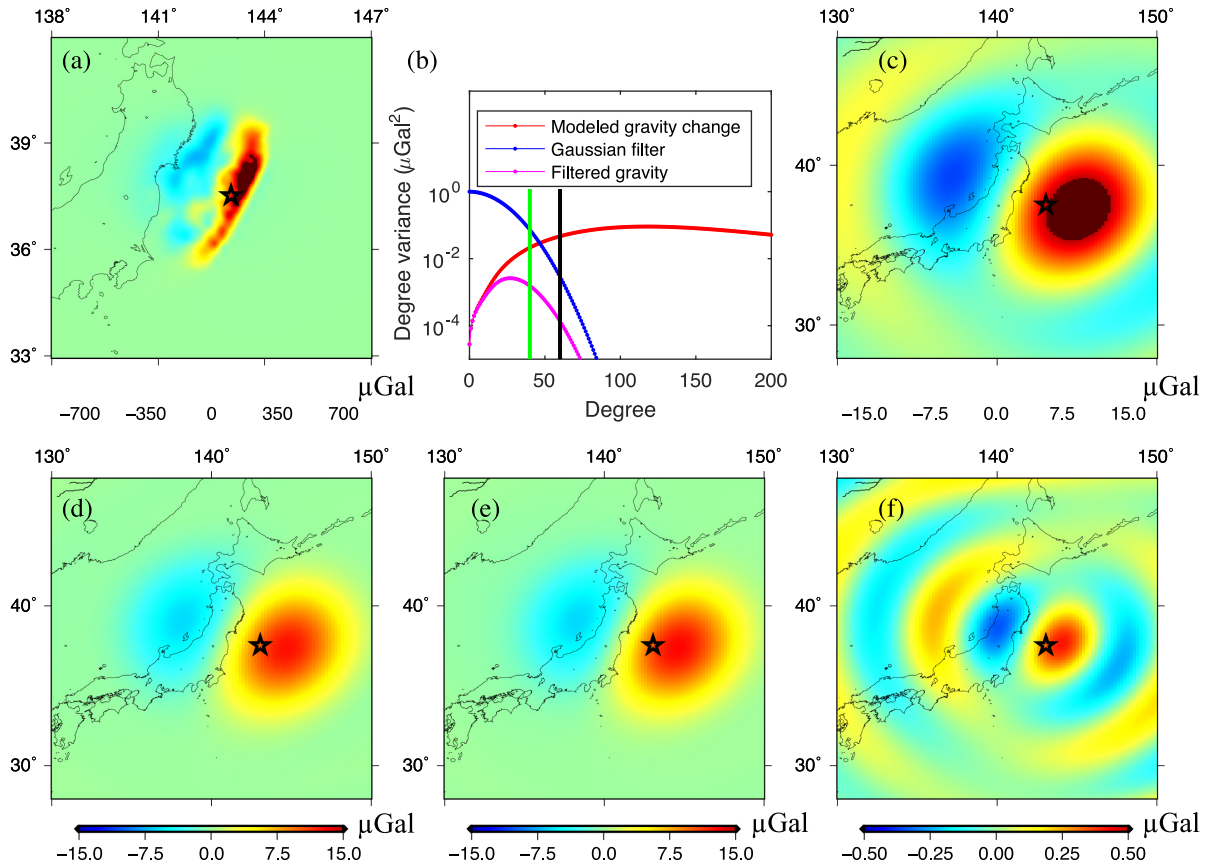

Figure 1. Effect of the spherical harmonic truncation and Gaussian filter. (a) Gravity change (μGal) at ocean floor (with no spherical harmonic truncation, at fixed space) due to solid Earth deformation (Dai *et al.* 2014). The slip distribution model is the sum of the coseismic slip model provided by Wei *et al.* (2012) and the 2 weeks of post-seismic slip model by Ozawa *et al.* (2011). The modelled gravity change is up to 1075 μGal. (b) The degree variance of the modelled gravity change (red line, μGal^2), the 300 km Gaussian filter (blue line, unitless) and the filtered gravity change (magenta, μGal^2). The vertical lines represent the locations of degree 40 (green) and degree 60 (black). (c) The gravity change (μGal) truncated to degree 40, up to 18.8 μGal. (d) The gravity change (μGal) truncated to degree 60 and then applied with 300 km Gaussian filter, up to 12.6 μGal. (e) The gravity change (μGal) at full resolution (a) applied with 300 km Gaussian filter, up to 12.9 μGal. (f) The residual (μGal) of (e) after subtraction of (d), up to 0.6 μGal.

or mass change signals by averaging the neighbouring signals using a weighting function. Although Gaussian filter largely reduces the higher degree signals, the difference between applying Gaussian filter to the full-resolution gravity change and the truncated gravity change is up to 0.6 μGal (Fig. 1f), or about 5 per cent of the maximum gravity change after 300 km Gaussian filtering (12.6 μGal). This demonstrates the amount of overestimation when compared to the smoothed GRACE gravity change if the same truncation is not applied in the modelling.

One drawback of Gaussian filter is that it largely reduces the power of high degree gravity signals, for example, reducing the degree variance by more than half for degrees higher than 30 for Gaussian filter with the smoothing radius of 300 km (Fig. 1b). Dai *et al.* (2016) elaborate an alternative way to mitigate the effect of stripes through the use of north component of gravity change, which is similar to the north component of the deflection of vertical (Sun & Zhou 2012) or gravity gradient (Wang *et al.* 2012c). The direct truncation is more preferable for coseismic deformation studies using GRACE, since the attenuation effect of Gaussian filter to high degrees would be avoided. Fig. 1(c) shows that the direct truncation yields gravity change with higher magnitude (18.8 μGal) when compared to that (12.6 μGal) using Gaussian filter. Nevertheless, direct truncation can cause ripple effect (Jekeli 1981) in the spatial domain. However, it does not affect the inversion of source parameters as long as the same truncation is applied in the forward modelling as that for GRACE data.

2.1 The effect of Earth's oblateness

This paper mainly focuses on one potential modelling deficiency, that is, the effect of the upward continuation of gravity change from the ocean floor to the Earth's mean equatorial radius, accounting for Earth's oblateness, which has not yet been discussed in previous publications for coseismic deformation studies. GRACE-derived gravity change is conventionally expanded as a series of spherical harmonics, computed at the Earth's mean equatorial radius R, that is, 6378.1363 km. However, the modelled gravity change corresponding to the solid Earth deformation is usually calculated on the solid Earth's surface, for example, the ocean floor for undersea earthquakes. A systematic bias will appear if comparing the model-predicted gravity change on the ocean floor directly with the GRACE-derived gravity change on R. The correct way is to transform the modelled gravity change at the ocean floor to the geopotential coefficients and then do upward continuation and obtained the gravity change on R.

Downloaded from https://academic.oup.com/gji/article-abstract/213/2/1297/4847898 by Bibliothek des Wissenschaftsparks Albert Einstein user on 08 January 2019

The relationship between the geopotential spherical harmonic coefficients and the north, east, down components of gravity change can be expressed as follows in the local north–east–down frame (Chen 2007):

$$g_N = -\frac{\partial T}{r\partial\theta} = \frac{GM}{R^2}\left(\sum_{n=2}^{\infty}\left(\frac{R}{r}\right)^{n+2} \times \sum_{m=0}^{n}\left(\Delta\overline{C}_{nm}\cos m\lambda + \Delta\overline{S}_{nm}\sin m\lambda\right)\overline{P}'_{nm}(\cos\theta)\sin\theta\right), \quad (1)$$

$$g_E = \frac{1}{r\sin\theta}\frac{\partial T}{\partial\lambda} = \frac{GM}{R^2\sin\theta}\left(\sum_{n=2}^{\infty}\left(\frac{R}{r}\right)^{n+2} \times \sum_{m=0}^{n} m\left(-\Delta\overline{C}_{nm}\sin m\lambda + \Delta\overline{S}_{nm}\cos m\lambda\right)\overline{P}_{nm}(\cos\theta)\right), \quad (2)$$

$$g_D = -\frac{\partial T}{\partial r} = \frac{GM}{R^2}\left(\sum_{n=2}^{\infty}(n+1)\left(\frac{R}{r}\right)^{n+2} \times \sum_{m=0}^{n}\left(\Delta\overline{C}_{nm}\cos m\lambda + \Delta\overline{S}_{nm}\sin m\lambda\right)\overline{P}_{nm}(\cos\theta)\right), \quad (3)$$

where g_N, g_E, g_D, are the north, east and down (radial) components of the gravity change, respectively. T is the geopotential change, which can be expressed as

$$T = \frac{GM}{R}\left(\sum_{n=2}^{\infty}\sum_{m=0}^{n}\left(\frac{R}{r}\right)^{n+1} \times \left(\Delta\overline{C}_{nm}\cos m\lambda + \Delta\overline{S}_{nm}\sin m\lambda\right)\overline{P}_{nm}(\cos\theta)\right), \quad (4)$$

where GM is the gravitational constant, n and m are the degree and order, respectively, and r, θ and λ are the local coordinates of any grid point around the fault area. $\overline{P}_{nm}$ is the fully normalized associated Legendre function (Wahr *et al.* 1998):

$$\bar{P}_{nm}(x) = \sqrt{(2-\delta_{m0})(2n+1)\frac{(n-m)!}{(n+m)!}} \times \frac{(1-x^2)^{\frac{m}{2}}}{2^n n!}\frac{d^{n+m}}{dx^{n+m}}(x^2-1)^n, \quad (5)$$

where $x = \cos\theta$, δ_{m0} is a Delta function, which equals to 1 only when m equals 0 and it is 0 otherwise. $\bar{P}'_{nm}(cos\theta)$ is the derivative of $\bar{P}_{nm}(x)$ with respect to x. $\bar{P}_{nm}$ can be calculated using the recursive formula as given in (Jekeli 1996), and $\bar{P}'_{nm}$ can be computed using the recursive formula in Tscherning *et al.* (1983). It is worth mentioning that $\Delta\overline{C}_{nm}$ and $\Delta\overline{S}_{nm}$ are the normalized spherical harmonic coefficient change defined at the Earth's mean equatorial radius R according to the data product standard documentation, from the University of Texas Center for Space Research, Jet Propulsion Laboratory/California Institute of Technology, and GeoForschungsZentrum Potsdam.

The above eq. (3) is used to get the band-limited spherical harmonic coefficients from the slip-predicted gravity change. Given the Earth density distribution model, we assume the gravity change is only caused by coseismic deformation of solid Earth corresponding to a rupture. Based on the dislocation theory in a layered half-space (Wang *et al.* 2006), the gravity change responding to the solid Earth deformation can be evaluated on a regular grid on a sphere, where the far-field gravity change (e.g. 20° away from the fault area) is set to zero. We emphasize that the radial coordinate for all grid points should be the geocentric distance of the local ocean floor over the fault area, r_s. If the Earth's mean equatorial radius R is erroneously used, instead of r_s as the radial coordinate of the modelled gravity change, it will cause systematic errors. Since the gravitational potential is harmonic in free space exterior to a sphere that contains all the masses (Jekeli 2007), the above eqs (1)–(4) are valid outside the sphere of radius r_s ($r > r_s$), and eq. (3) can be used for the upward continuation of coseismic gravity change from r_s to R. Specifically, we can expand g_D at r_s as (Guo & Shum 2009):

$$g_D = \frac{GM}{R^2}\left(\sum_{n=2}^{\infty}\sum_{m=0}^{n}\left(\Delta\hat{C}_{nm}\cos m\lambda + \Delta\hat{S}_{nm}\sin m\lambda\right)\overline{P}_{nm}(\cos\theta)\right). \quad (6)$$

Let $r = r_s$ in eq. (3), we have the relation between $\Delta\overline{C}_{nm}$, $\Delta\overline{S}_{nm}$ and $\Delta\hat{C}_{nm}$, $\Delta\hat{S}_{nm}$:

$$\begin{Bmatrix}\Delta\overline{C}_{nm}\\ \Delta\overline{S}_{nm}\end{Bmatrix} = \frac{1}{n+1}\left(\frac{r_s}{R}\right)^{n+2}\begin{Bmatrix}\Delta\hat{C}_{nm}\\ \Delta\hat{S}_{nm}\end{Bmatrix}. \quad (7)$$

The model-predicted coefficients change $\Delta\overline{C}_{nm}$, $\Delta\overline{S}_{nm}$ can then be compared commensurately with GRACE Level 2 products, and they can be directly applied to eqs (1)–(4).

The computation of the radial distance (r_s) of the more realistic solid Earth surface, that is, considering the Earth's oblateness, over a fault area (Dai 2015) is described here. Given the geodetic latitude and longitude coordinates of the slip location, we first compute the geocentric distance of the fault location projected on the Earth ellipsoid (Dai 2015). The geocentric distance on the WGS84 (World Geodetic System 1984) ellipsoid over the fault location can be computed as

$$R_{\text{ellipsoid}} = \sqrt{x^2+z^2}. \quad (8)$$

where, $x = a\cos\varphi/\sqrt{1-e^2\sin^2\varphi}$, $z = a(1-e^2)\sin\varphi/\sqrt{1-e^2\sin^2\varphi}$, φ is the geodetic latitude of the coseismic slip, a is the semi-major axis of the WGS84 ellipsoid and e is the first eccentricity of the Earth ellipsoid. Considering the variation of $R_{\text{ellipsoid}}$ along the latitude in a region, we adopt the Global Centroid Moment Tensor Project (GCMT) centroid location as the location of a fault plane.

The geocentric radial distance of the solid Earth surface over the fault area, r_s, can be computed by adding the elevation of the Earth surface (topography/bathymetry) to the local geoid's geocentric distance (e.g. 6370 km, for the fault area of 2011 Tohoku earthquake). The geocentric distance of the local geoid at the fault region is: $R_{\text{Geoid}} = R_{\text{ellipsoid}} + N$, where N is the geoid undulation. Neglecting the geoid undulation, which is less than ~107 meter globally (Pavlis *et al.* 2008), the geocentric distance of the Earth surface, r_s, would be

$$r_s = R_{\text{Geoid}} + h_{\text{elev}} = R_{\text{ellipsoid}} + N + h_{\text{elev}} \approx R_{\text{ellipsoid}} + h_{\text{elev}}, \quad (9)$$

where h_{elev} is the elevation of the solid Earth surface, for example, ocean floor, which can be extracted from the topography and bathymetry data in CRUST2.0 model (Bassin *et al.* 2000). Considering the bathymetric variation along fault planes, which are usually located along trench areas, we use the average elevation of seafloor over a fault area as h_{elev}.

Downloaded from https://academic.oup.com/gji/article-abstract/213/2/1297/4847898 by Bibliothek des Wissenschaftsparks Albert Einstein user on 08 January 2019

Table 1. The upward continuation of the model-predicted g_D change for five undersea earthquakes.

	Latitude	h_{elev} (km)	r_s (km)	Max($\|g_D(r_s)\|$) (μGal)	Max($\|g_D(R)\|$) (μGal)	rd
The 2004 Sumatra–Andaman (M_w 9.2) earthquake	1.67° N	–1.8	6376.3	46.4	45.8	1%
The 2011 Tohoku (M_w 9.0) earthquake	37.52° N	–3.9	6366.1	51	47	9%
The 2010 Maule (M_w 8.8) earthquake	35.98° S	–1.3	6369.4	28.4	26.7	6%
The 2012 Indian Ocean (M_w 8.6 and M_w 8.2) earthquakes*	2.35° N	–4.0	6374.1	3.4	3.3	3%
The 2007 Bengkulu (M_w 8.5) earthquake*	3.78° S	–1.3	6376.8	2.59	2.57	1%

The g_D change is computed up to the maximum spherical harmonic degree of 60.
* For the 2012 Indian Ocean earthquakes and the 2007 Bengkulu earthquake, the g_D change is computed up to the maximum spherical harmonic degree of 40, which is the maximum degree that can be reliably retrieved from GRACE data (Dai *et al.* 2016).
Max($|g_D(R)|$) is the maximal magnitude of the coseismic g_D change computed at the radial distance, R; Max($|g_D(r_s)|$) is the same, except the g_D change is computed at the ocean floor with the radial distance of r_s. The relative difference of the maximum coseismic gravity change is defined as, rd = Max($|g_D(r_s)|$)/Max($|g_D(R)|$) − 1. The column of latitude denotes the GCMT centroid latitude of each earthquake, and h_{elev} is the seafloor elevation averaged over the fault area.

3 NUMERICAL EVALUATION ON THE UPWARD CONTINUATION OF GRAVITY CHANGE

Here we numerically evaluate the systematic error caused by ignoring the upward continuation of modelled gravity change from ocean floor r_s to R. We evaluate the difference by comparing the magnitude of model-predicted g_D change on r_s with that on R. For simplicity, the comparison is only carried out for the gravity change associated with the solid Earth deformation, and the conclusion are expected to be the same for the total gravity change by the solid Earth deformation, the ocean response and the topographic effect. The upward continuation of the slip-model-predicted g_D change for five undersea earthquakes is conducted (Table 1), showing that the maximum magnitude of the coseismic g_D change computed at the Earth's mean equatorial radius, R, is smaller than that computed at the ocean floor, r_s. As shown in Table 1, the effect of the upward continuation is small for those earthquakes close to the equator, with the relative difference of only 1 per cent for the 2004 Sumatra–Andaman earthquake (Chlieh *et al.* 2007) and the 2007 Bengkulu earthquake (Konca *et al.* 2008), and only 3 per cent for the 2012 Indian Ocean earthquakes (Yue *et al.* 2012). For the two middle latitude earthquakes, the 2011 Tohoku earthquake (Ozawa *et al.* 2011; Wei *et al.* 2012) and the 2010 Maule earthquake (Hayes 2010), due to their smaller geocentric distances (because of earth oblateness) at their fault areas compared to R, the effect of the upward continuation on g_D change is larger, with relative differences of 9 per cent and 6 per cent. The effect of the upward continuation on the magnitude of the modelled gravity change will directly affect the estimation of seismic moment during the source parameters inversion using GRACE data. For example, for the 2011 Tohoku earthquake, if neglecting the upward continuation of g_D change from the ocean floor to R, the model-predicted g_D change would be overestimated by 9 per cent (Table 1); hence, the magnitude of seismic moment will be underestimated by 9 per cent during the source parameters inversion using GRACE-observed gravity change because of the linear relationship between the observed gravity change and the inverted source parameters.

A simple formula, $(R/r_s)^{NMAX+2} - 1$, can be used as a rough approximation for initial evaluation of the effect of ignoring the upward continuation for any high frequency geophysical signal. As shown in eq. (7), the effect of upward continuation for the g_D change is mainly dominated by the factor, $(r_s/R)^{n+2}$. If ignored, it will introduce relative error of $(1 - (r_s/R)^{n+2})/((r_s/R)^{n+2}) = (R/r_s)^{n+2} - 1$, for a given degree n. For geophysical signals with high power at high frequencies, the magnitude of the signal may be roughly approximated with the maximum degree term. Then, its relative difference can be roughly approximated by $(R/r_s)^{NMAX+2} - 1$. Fig. 2 demonstrates the small difference between the approximated relative differences (yellow) with the estimated relative differences (red) (Table 1). Nevertheless, this simple approximation only holds when the geophysical signal has the highest power at or above the truncation degree NMAX of the Stokes coefficients.

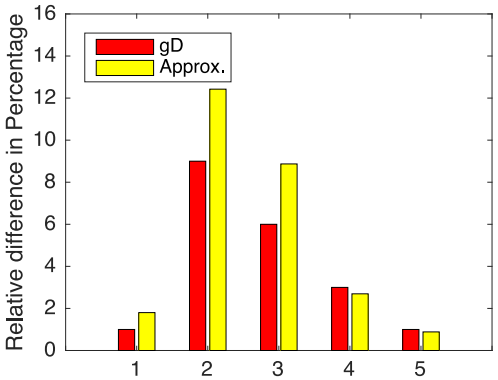

Figure 2. The relative differences for five recent undersea earthquakes (Table 1). Red is the estimated relative difference, and the yellow is the value calculated using the simple approximation formula.

We further extend our evaluation for higher degree gravity solutions. To show the effect of the upward continuation for gravity field solutions with different maximum degrees, we compute the peak value of the model-predicted g_D change, for the 2011 Tohoku earthquake, truncated at different degrees (Fig. 3). First, we can see that the model-predicted g_D change at the ocean floor (Fig. 3 top, red line) has increasing magnitude with the truncated degrees, up to 995 μGal truncated at degree 900, much higher than the peak value of 51 μGal truncated at degree 60, indicating the high power of the seismic signal at the high frequencies. The g_D change at R (Fig. 3 top, orange line) is systematically smaller than the g_D change at the ocean floor (Fig. 3 top, red line), with their relative difference (Fig. 3 bottom, red) increasing with truncation degrees. The relative difference between the g_D change at r_s and the g_D change at R is around 60 per cent (Fig. 3 bottom, red) when truncated at degree 900, and it is about 30 per cent when truncated at degree 240, which is the maximum degree for various gravity field models (e.g. ITG-Goce02, http://icgem.gfz-potsdam.de/ICGEM, Schall *et al.* 2014) by another satellite gravity gradiometry-GOCE measurements (Pail *et al.* 2011; Schall *et al.* 2014). Similar to the GRACE gravity field models, the GOCE gravity field models also use the mean equatorial radius of the Earth (6378.13646 km) for its spherical harmonic coefficients. Hence, for the study of the 2011 Tohoku earthquake using high de-

Downloaded from https://academic.oup.com/gji/article-abstract/213/2/1297/4847898 by Bibliothek des Wissenschaftsparks Albert Einstein user on 08 January 2019

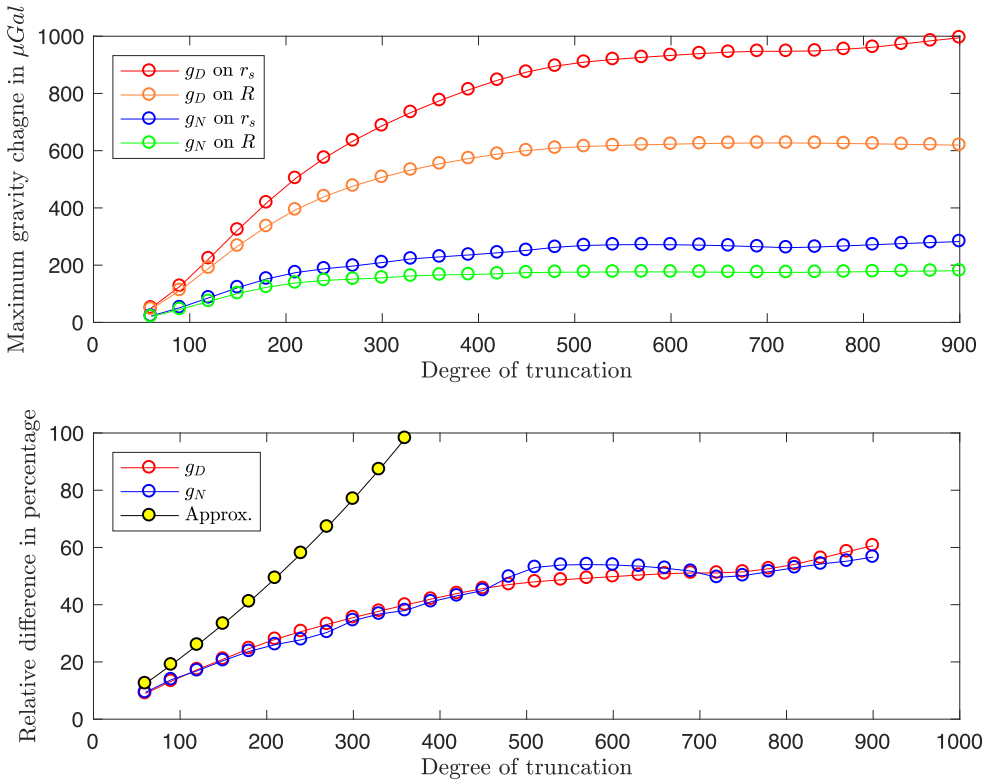

Figure 3. The effect of the upward continuation as a function of the degree of truncation, for the 2011 Tohoku earthquake. Top: the maximum north (g_N) and down (g_D) component of gravity change corresponding to solid Earth deformation as a function of the truncated degree, calculated at R and at the ocean floor, r_s. Bottom: the relative difference for g_N, g_D change. The slip distribution model is the sum of the coseismic slip model provided by Wei *et al.* (2012) and the 2 weeks of post-seismic slip model by Ozawa *et al.* (2011).

gree gravity field solutions (e.g. maximum degree 240), this effect of the upward continuation of the model-predicted gravity signal from the ocean floor to R could be significant (30 per cent). For the north component of gravity change (blue line, Fig. 3 bottom), the effect of the upward continuation is at the same magnitude as that for the g_D change.

The yellow line (Fig. 3) gives the value using the approximated formula, which only roughly agrees with the relative difference (red line) for degrees below 100. Above degree 100, the approximation deviates from the estimated relative difference. The reason is that the localized degree variance (Wieczorek & Simons 2005; Simons *et al.* 2006) of the coseismic gravity change drops at around degree 100 (Fig. 4), which indicates that the degree NMAX term above degree 100 can no longer approximate the magnitude of the signal. Nevertheless, we should be aware that the evaluation of the effect of the upward continuation (Fig. 3) and the degree variance (Fig. 4) highly relies on the coseismic slip model (Wei *et al.* 2012), which is resolved with some smoothing conditions added during their inversion, for example, the spline distribution among patches, or the criteria of least discrepancy between neighbour patches. This implies that potentially the real coseismic slip signal could have even higher power at the high degrees than that shown in Fig. 4, which implies that the effect of the upward continuation neglecting Earth's oblateness (Fig. 3, bottom) could be larger for real coseismic signals.

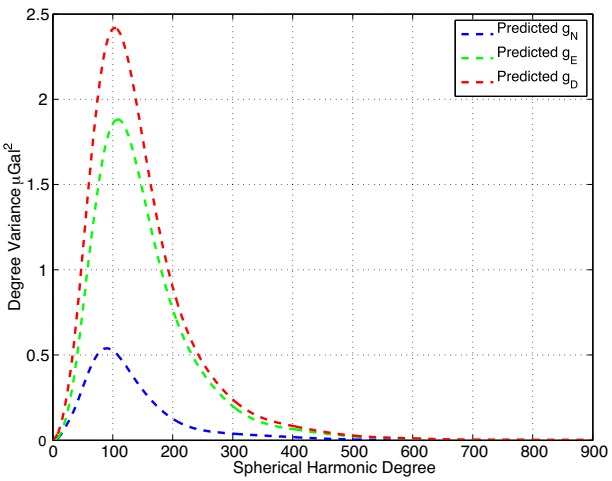

Figure 4. The localized degree variance for the model-predicted g_N, g_E, g_D change. The slip distribution model is the sum of the coseismic slip model (Wei *et al.* 2012) and the 2 weeks of post-seismic slip model (Ozawa *et al.* 2011). g_E is the east component of gravity change.

4 DISCUSSION AND CONCLUSIONS

This paper discusses several modelling issues in the earthquake source model inversion studies using long-wavelength satellite-based gravity data. We particularly demonstrate the effect of spherical harmonic truncation, showing that the difference between applying Gaussian filter to the full-resolution gravity change and to the truncated gravity change is about 5 per cent of the maximum gravity change, and that the direct truncation without Gaussian filter is more preferable for coseismic deformation studies using GRACE gravimetry data. Our main focus is the systematic bias in the modelling of the GRACE-commensurable gravity

Downloaded from https://academic.oup.com/gji/article-abstract/213/2/1297/4847898 by Bibliothek des Wissenschaftsparks Albert Einstein user on 08 January 2019

change, caused by ignoring the upward continuation of the gravity change from a more realistic solid Earth's surface (e.g. ocean floor) to the Earth's mean equatorial radius, for five recent large earthquakes. Ignoring this effect may lead to biases when comparing the GRACE-observed gravity change with the slip-model-predicted gravity change, and consequently, yielding biases in the estimated seismic moment during earthquakes source model inversion using GRACE data. We found that the effect of the upward continuation is non-negligible (6 per cent∼9 per cent) for middle latitude earthquakes, and the effect is small (1 per cent to 3 per cent) for those earthquakes close to the equator. A simple formula, $(R/r_s)^{\mathrm{NMAX}+2} - 1$, can be used as a rough approximation for initial evaluation of this effect on any high frequency geophysical signal. In addition, the effect is more significant for higher degree gravity field solutions for future missions. For example, for scales more commensurate with a seismic displacement model, a gravity field product up to degree 240, if ignoring the difference between the Earth's mean equatorial radius and the local geocentric distance at the solid Earth's surface during the forward modelling procedure, the model-predicted gravity change can be overestimated by 30 per cent for the 2011 Tohoku earthquake, which means that the inverted seismic moment may be systematically underestimated by 30 per cent.

ACKNOWLEDGEMENTS

We acknowledge Frederik Simons, Princeton University, for useful discussions and for providing his open software on localized spectral analysis. We acknowledge Shengji Wei, Han Yue, David Sandwell, and authors of the eQuake-RC, http://equake-rc.info, for providing various coseismic and post-seismic slip models. We thank seismologists and geodesists at the U.S. Geological Survey and other institutes for providing various data associated with the earthquakes chosen in this study and the associated inverted slide models. This research is primarily supported by the National Aeronautics and Space Administration (NASA)'s Earth and Space Science Fellowship (ESSF) Program (Grant NNX12AO06H), and Earth Surface Interior Program (Grant NNX14AP98G); and by National Natural Science Foundation of China (Grants 41584016 and 41374020). Some figures in this paper were generated using the Generic Mapping Tools (GMT; Wessel & Smith 1991). The computing resources in this work are partially supported by a generous allocation of supercomputing cycles from the Ohio Supercomputer Center (http://www.osc.edu). The code developed in this study is available at https://github.com/Chunli-Dai/GRACEEarthquakeModeling. We thank Editor Bert Vermeersen and two anonymous reviewers for their constructive comments.

REFERENCES

Álvarez, O., Nacif, S., Gimenez, M., Folguera, A. & Braitenberg, C., 2014. GOCE derived vertical gravity gradient delineates great earthquake rupture zones along the Chilean margin, *Tectonophysics,* **622**, 198–215.

Bassin, C., Laske, G. & Masters, G., 2000. The current limits of resolution for surface wave tomography in North America, *EOS, Trans. Am. geophys. Un.,* **81**, F897.

Broerse, D., Vermeersen, L., Riva, R. & van der Wal, W., 2011. Ocean contribution to co-seismic crustal deformation and geoid anomalies: application to the 2004 December 26 Sumatra–Andaman earthquake, *Earth planet. Sci. Lett.,* **305**(3–4), 341–349.

Broerse, T., Riva, R. & Vermeersen, B., 2014. Ocean contribution to seismic gravity changes: the sea level equation for seismic perturbations revisited, *Geophys. J. Int.,* **199**(2), 1094–1109.

Cambiotti, G., Bordoni, A., Sabadini, R. & Colli, L., 2011. GRACE gravity data help constraining seismic models of the 2004 Sumatran earthquake, *J. geophys. Res.,* **116**(B10), B10403, doi:10.1029/2010JB007848.

Cambiotti, G. & Sabadini, R., 2012. A source model for the great 2011 Tohoku earthquake ($M_w = 9.1$) from inversion of GRACE gravity data, *Earth planet. Sci. Lett.,* **335–336**, 72–79.

Cambiotti, G. & Sabadini, R., 2013. Gravitational seismology retrieving Centroid-Moment-Tensor solution of the 2011 Tohoku earthquake, *J. geophys. Res.,* **118**(1), 183–194.

Chen, Y., 2007. Recovery of terrestrial water storage change from low–low satellite-to-satellite tracking, Rep. 485, Dep. of Geod. Sci. and Surv., Ohio State Univ., Columbus.

Chlieh, M. *et al.*, 2007. Coseismic Slip and Afterslip of the great M_w 9.15 Sumatra–Andaman earthquake of 2004, *Bull. seism. Soc. Am.,* **97**(1A), S152–S173.

Dai, C., Shum, C.K., Wang, R., Wang, L., Guo, J., Shang, K. & Tapley, B., 2014. Improved constraints on seismic source parameters of the 2011 Tohoku earthquake from GRACE gravity and gravity gradient changes, *Geophys. Res. Lett.,* **41**(6), 1929–1936.

Dai, Chunli 2015. Source Parameters Inversion for Recent Large Undersea Earthquakes from GRACE Data*,* OSU Report No. 510, Div. of Geodetic Sciences, School of Earth Sciences, The Ohio State University, Columbus, OH, USA.

Dai, C., Shum, C., Guo, J., Shang, K., Tapley, B. & Wang, R., 2016. Improved source parameter constraints for five undersea earthquakes from north component of GRACE gravity and gravity gradient change measurements, *Earth planet. Sci. Lett.,* **443**, 118–128.

de Linage, C., Rivera, L., Hinderer, J., Boy, J.-P., Rogister, Y., Lambotte, S. & Biancale, R., 2009. Separation of coseismic and post-seismic gravity changes for the 2004 Sumatra–Andaman earthquake from 4.6 yr of GRACE observations and modelling of the coseismic change by normal-modes summation, *Geophys. J. Int.,* **176**(3), 695–714.

Dong, Jie, Sun, W., Zhou, X. & Wang, R., 2016. An analytical approach to estimate curvature effect of coseismic deformations, *Geophys. J. Int.,* **206**(2), 1327–1339.

Fuchs, M.J., Bouman, J., Broerse, T., Visser, P. & Vermeersen, B., 2013. Observing coseismic gravity change from the Japan Tohoku-Oki 2011 earthquake with GOCE gravity gradiometry, *J. geophys. Res.,* **118**(10), 5712–5721.

Guo, J.Y. & Shum, C. K., 2009. Application of the cos-Fourier expansion to data transformation between different latitude–longitude grids, *Comput. Geosci.,* **35**(7), 1439–1444.

Guo, J.Y., Duan, X.J. & Shum, C.K., 2010. Non-isotropic Gaussian smoothing and leakage reduction for determining mass changes over land and ocean using GRACE data, *Geophys. J. Int.,* **181**(1), 290–302.

Han, S.-C., Shum, C., Bevis, M., Ji, C. & Kuo, C., 2006. Crustal dilatation observed by GRACE after the 2004 Sumatra–Andaman earthquake, *Science,* **313**(5787), 658–662.

Han, S.-C., Sauber, J., Luthcke, S., Ji, C. & Pollitz, F., 2008. Implications of postseismic gravity change following the great 2004 Sumatra–Andaman earthquake from the regional harmonic analysis of GRACE intersatellite tracking data, *J. geophys. Res.,* **113**(B11), B11413, doi:10.1029/2008JB005705.

Han, S.-C., Sauber, J. & Luthcke, S., 2010. Regional gravity decrease after the 2010 Maule (Chile) earthquake indicates large-scale mass redistribution, *Geophys. Res. Lett.,* **37**(23), doi:10.1029/2010GL045449.

Han, S.-C., Sauber, J. & Riva, R., 2011. Contribution of satellite gravimetry to understanding seismic source processes of the 2011 Tohoku-Oki earthquake, *Geophys. Res. Lett.,* **38**(24), doi:10.1029/2011GL049975.

Han, S.-C., Riva, R., Sauber, J. & Okal, E., 2013. Source parameter inversion for recent great earthquakes from a decade-long observation of global gravity fields, *J. geophys. Res.,* **118**(3), 1240–1267.

Han, S.C., Sauber, J. & Pollitz, F., 2014. Broadscale postseismic gravity change following the 2011 Tohoku-Oki earthquake and implication for

Downloaded from https://academic.oup.com/gji/article-abstract/213/2/1297/4847898 by Bibliothek des Wissenschaftsparks Albert Einstein user on 08 January 2019

deformation by viscoelastic relaxation and afterslip, *Geophys. Res. Lett.,* **41**(16), 5797–5805.

Hayes, G., 2010. 'Finite fault model, updated results of the Feb. 27, 2010 M_w 8.8 Maule, Chile earthquake'. Available at: http://earthquake.usgs.gov/earthquakes/eqinthenews/2010/us2010tfan/finite_fault.php. (Last accessed: January 12, 2015).

Heki, K. & Matsuo, K., 2010. Coseismic gravity changes of the 2010 earthquake in central Chile from satellite gravimetry, *Geophys. Res. Lett.,* **37**(24), doi:10.1029/2010GL045335.

Jekeli, C., 1981. Alternative methods to smooth the Earth's gravity field, Rep. 327, Dep. of Geod. Sci. and Surv., Ohio State Univ., Columbus.

Jekeli, C., 1996. Spherical harmonic analysis, aliasing, and filtering. *J. Geod.,* **70**(4), 214–223.

Jekeli, C., 2007. Potential theory and static gravity field of the Earth, in *Treatise on Geophysics,* Vol. 3, pp. 11–42, ed. Schubert, G., Elsevier.

Konca, A.O. *et al.*, 2008. Partial rupture of a locked patch of the Sumatra megathrust during the 2007 earthquake sequence, *Nature,* **456**(7222), 631–635.

Li, J. & Chen, J., 2013. Effect of topography on coseismic gravity changes and verification from GRACE, in *Asia-Pacific Space Geodynamics (APSG) Symposium,* the Ohio State University, Columbus, Ohio, USA, October 14–17, 2013.

Li, Jin & Shen, W.B., 2015. Monthly GRACE detection of coseismic gravity change associated with 2011 Tohoku-Oki earthquake using northern gradient approach, *Earth Planets Space,* **67**(1), 1, doi:10.1186/s40623-015-0188-0.

Li, J., Chen, J.L. & Wilson, C.R., 2016. Topographic effects on co-seismic gravity change for the 2011 Tohoku-Oki earthquake and comparison with GRACE, *J. geophys. Res.,* **121**, 5509–5537.

Li, J., Chen, J., Li, Z., Wang, S.Y. & Hu, X., 2017. Ellipsoidal Correction in GRACE surface mass change estimation, *J. geophys. Res.,* **122**, 9437–9460.

Luthcke, S.B., Sabaka, T.J., Loomis, B.D., Arendt, A.A., McCarthy, J.J. & Camp, J., 2013. Antarctica, Greenland and Gulf of Alaska land-ice evolution from an iterated GRACE global mascon solution, *J. Glaciol.,* **59**(216), 613–631, https://doi.org/10.3189/2013JoG12J147.

Matsuo, K. & Heki, K., 2011. Coseismic gravity changes of the 2011 Tohoku-Oki earthquake from satellite gravimetry, *Geophys. Res. Lett.,* **38**(7), doi:10.1029/2011GL049018.

Ogawa, R. & Heki, K., 2007. Slow postseismic recovery of geoid depression formed by the 2004 Sumatra–Andaman earthquake by mantle water diffusion, *Geophys. Res. Lett.,* **34**(6), L06313, doi:10.1029/2007GL029340.

Ozawa, S., Nishimura, T., Suito, H., Kobayashi, T., Tobita, M. & Imakiire, T., 2011. Coseismic and postseismic slip of the 2011 magnitude-9 Tohoku-Oki earthquake, *Nature,* **475**(7356), 373–376.

Pail, R., Bruinsma, S., Migliaccio, F., Förste, C., Goiginger, H., Schuh, W. & Höck, E. *et al.*, 2011. First GOCE gravity field models derived by three different approaches, *J. Geod.,* **85**(11), 819–843.

Panet, I., Pollitz, F.F., Mikhailov, V., Diament, M., Banerjee, P. & Grijalva, K., 2010. Upper mantle rheology from GRACE and GPS postseismic deformation after the 2004 Sumatra–Andaman earthquake, *Geochem. Geophys. Geosyst.,* **11**(6), doi:10.1029/2009GC002905.

Pavlis, N.K., Holmes, S.A., Kenyon, S.C. & Factor, J.K., 2008. An earth gravitational model to degree 2160: EGM2008, *presented at the 2008 General Assembly of the European Geosciences Union,* Vienna, Austria, April 13–18, 2008.

Pollitz, F.F., 1996. Coseismic deformation from earthquake faulting on a layered spherical Earth, *Geophys. J. Int.,* **125**(1), 1–14.

Rummel, R., Gruber, T. & Koop, R., 2004. High level processing facility for GOCE: products and processing strategy, in *Proceedings of the 2nd International GOCE User Workshop,* ESA-SP569, pp. 8–10.

Schall, J., Eicker, A. & Kusche, J., 2014. The ITG-Goce02 gravity field model from GOCE orbit and gradiometer data based on the short arc approach, *J. Geod.,* **88**(4), 403–409.

Simons, F., Dahlen, F. & Wieczorek, M., 2006. Spatiospectral concentration on a Sphere, *SIAM Rev.,* **48**(3), 504–536.

Sun, W. & Okubo, S., 1993. Surface potential and gravity changes due to internal dislocations in a spherical earth-I. Theory for a point dislocation, *Geophys. J. Int.,* **114**(3), 569–592.

Sun, W. & Zhou, X., 2012. Coseismic deflection change of the vertical caused by the 2011 Tohoku-Oki earthquake (M_w 9.0), *Geophys. J. Int.,* **189**(2), 937–955.

Swenson, S. & Wahr, J., 2002. Estimated effects of the vertical structure of atmospheric mass on the time-variable geoid, *J. geophys. Res.,* **107**(B9), ETG 4-1–ETG 4-11.

Tanaka, Y. & Heki, K., 2014. Long- and short-term postseismic gravity changes of megathrust earthquakes from satellite gravimetry, *Geophys. Res. Lett.,* **41**(15), 5451–5456.

Tanaka, Y., Heki, K., Matsuo, K. & Shestakov, N. V., 2015. Crustal subsidence observed by GRACE after the 2013 Okhotsk deep-focus earthquake, *Geophys. Res. Lett.,* **42**(9), 3204–3209.

Tapley, B.D., Bettadpur, S., Ries, J.C., Thompson, P.F. & Watkins, M.M., 2004. GRACE measurements of mass variability in the Earth system, *Science,* **305**(5683), 503–505.

Tscherning, C.C., Rapp, R.H. & Goad, C., 1983. A comparison of methods for computing gravimetric quantities from high degree spherical harmonic expansions, *Manuscr. Geod.,* **8**, 249–272.

Wahr, J., Molenaar, M. & Bryan, F., 1998. Time variability of the Earth's gravity field: Hydrological and oceanic effects and their possible detection using GRACE, *J. geophys. Res.,* **103**(B12), 30205–30229.

Wang, R., Lorenzo-Martin, F. & Roth, F., 2006. PSGRN/PSCMP—a new code for calculating co- and post-seismic deformation, geoid and gravity changes based on the viscoelastic-gravitational dislocation theory, *Comput. Geosci.,* **32**(4), 527–541.

Wang, L. *et al.*, 2012a. Coseismic slip of the 2010 M_w 8.8 Great Maule, Chile, earthquake quantified by the inversion of GRACE observations, *Earth planet. Sci. Lett.,* **335–336**, 167–179.

Wang, L., Shum, C., Simons, F., Tapley, B. & Dai, C., 2012b. Coseismic and postseismic deformation of the 2011 Tohoku-Oki earthquake constrained by GRACE gravimetry, *Geophys. Res. Lett.,* **39**, L07301, doi:10.1029/2012GL051104.

Wang, L., Shum, C. & Jekeli, C., 2012c. Gravitational gradient changes following the 2004 December 26 Sumatra–Andaman earthquake inferred from GRACE, *Geophys. J. Int.,* **191**(3), 1109–1118.

Watkins, M.M., Wiese, D.N., Yuan, D.N., Boening, C. & Landerer, F.W., 2015. Improved methods for observing Earth's time variable mass distribution with GRACE using spherical cap mascons, *J. geophys. Res.,* **120**(4), 2648–2671.

Wei, Shengji, Graves, R., Helmberger, D., Avouac, J.P. & Jiang, J., 2012. Sources of shaking and flooding during the Tohoku-Oki earthquake: A mixture of rupture styles, *Earth planet. Sci. Lett.,* **333–334**, 91–100.

Wessel, P. & Smith, W.H., 1991. Free software helps map and display data, *EOS, Trans. Am. geophys. Un.,* **72**(41), 441–446.

Wieczorek, M.A. & Simons, F.J., 2005. Localized spectral analysis on the sphere, *Geophys. J. Int.,* **162**(3), 655–675.

Yue, H., Lay, T. & Koper, K., 2012. En échelon and orthogonal fault ruptures of the 11 April 2012 great intraplate earthquakes, *Nature,* **490**(7419), 245–249.

Zhou, X., Sun, W., Zhao, B., Fu, G., Dong, J. & Nie, Z., 2012. Geodetic observations detecting coseismic displacements and gravity changes caused by the M_w = 9.0 Tohoku-Oki earthquake, *J. geophys. Res.,* **117**(B5), doi:10.1029/2011JB008849.

Downloaded from https://academic.oup.com/gji/article-abstract/213/2/1297/4847898 by Bibliothek des Wissenschaftsparks Albert Einstein user on 08 January 2019